CO$_2$ and CH$_4$ fluxes from standing dead trees in a northern conifer forest

Christian Hettwer [1], Kathleen Savage [2], Andrew Ouimette [3], Jay Wason [1], Roel Ruzol [1], Shawn Fraver [1]

[1] School of Forest Resources, University of Maine, Orono, ME 04469, USA
[2] Woodwell Climate Research Center, Falmouth, MA 02540, USA
[3] USDA Forest Service, Northern Research Station, Durham, NH 03825, USA

Correspondence to: Christian Hettwer (christian.hettwer@maine.edu)

Abstract. Representing 15 – 20% of aboveground biomass in forests, deadwood is an important, yet understudied, component of ecosystem greenhouse gas (GHG) fluxes. In particular, standing dead trees (snags) can serve as conduits for the atmospheric flux of carbon dioxide (CO_2) and methane (CH_4), with fluxes varying according to environmental conditions. We measured CO_2 and CH_4 fluxes from six snags along an upland-to-wetland gradient at Howland Research Forest (Maine, USA) with measurements made every two weeks from April to November 2024. Using nonlinear models, we quantified flux responses to environmental predictors including soil moisture, soil temperature, and air temperature. Gas fluxes increased with increasing temperature, yet CO_2 flux peaked at moderate soil moisture ($\sim 30\%$), while CH_4 peaked at the highest moisture levels. CH_4 fluxes were overwhelmingly net positive, confirming that snags are important pathways for wetland gas emission. CH_4 flux was relatively insensitive under low soil moisture and temperature but increased with rising soil temperature when soil moisture was high, suggesting that methanogenesis depends on anaerobic moisture conditions. Results also suggest that CO_2 flux co-varied with CH_4 flux from snags, with decreases in CO_2 flux associated with increases in CH_4 flux. As soil moisture increased, a pronounced shift in gas fluxes (from CO_2 to CH_4 emission) occurred at $\sim 60\%$ soil moisture. Compared to other substrates at the site, including soils, living trees, and various deadwood, snags were the largest emitters of CO_2 and second-largest emitters of CH_4. We present direct measurements of gas exchange from snags along a moisture and temperature gradient, providing new insights into CO_2 and CH_4 fluxes from snags.

| Deleted: suggesting |
| Deleted: , |
| Deleted: These results, which align with those from previous studies establishing anaerobic moisture thresholds and provide new insights into CO_2 and CH_4 fluxes from snags, present direct measurements of gas exchange from snags along a moisture and temperature gradient. |

1 Introduction

Deadwood can represent as much as 20% of aboveground biomass in forests, thereby contributing significantly to global carbon dynamics (Komposch et al., 2022; Russell et al., 2015; Woodall et al., 2015). Among deadwood components, standing dead trees, or snags, are particularly important because they remain upright for years, decaying and releasing gases slower than other types of deadwood (Hararuk et al., 2020; Onega and Eickmeier, 1991). This is particularly important in forests with high snag densities or recent disturbances, where deadwood volumes are elevated (Kipping et al., 2022; Yatskov et al., 2022). Snags also influence carbon flux dynamics by serving as a conduit for atmospheric flux of carbon dioxide (CO_2) and methane (CH_4), transporting soil-generated gases and also producing within-stem gases (Carmichael et al., 2018). Relatively few studies have addressed greenhouse gas (GHG) fluxes from snags, despite their acknowledged importance in ecosystem functioning and forest carbon dynamics.

Snags emit CO_2 as the result of heterotrophic respiration. As fungi decompose wood, environmental factors, including soil moisture and temperature, influence CO_2 flux rates (Mukhortova et al., 2021; Noh et al., 2019). CO_2 flux from snags is positively influenced by temperature, as warmer conditions generally enhance decomposition (Renninger et al., 2014). While moisture is known to have a positive relationship with CO_2 flux from deadwood (Olajuyigbe et al., 2012), excessive moisture can limit oxygen diffusion in snag stems, reducing CO_2 emissions (Oberle et al., 2018). Snag CO_2 emissions (per unit area) are typically smaller in magnitude than those from soils; however, emissions from the two sources are often positively correlated, as both arise from similar biological processes and environmental drivers (Perreault et al., 2021).

Even less well understood is CH_4 flux from snags, which can arise through two primary pathways: passive transport of soil-generated CH_4 through the stem and *in situ* production within the stem.

In water-saturated soils, methanogenic archaea anaerobically produce CH_4, primarily by reducing CO_2 (Conrad, 2020). Internal conduits, particularly in trees with compromised xylem structure, can transport CH_4 upward through the stem to be diffused to the atmosphere (Keppler et al., 2006; Pangala et al., 2013). This mechanism is well documented in living trees (Barba et al., 2019; Pangala et al., 2015), and emerging evidence suggests that snags can similarly serve as conduits for soil-emitted CH_4 (Carmichael et al. 2018). However, because snags have the potential to host both methanogenic (CH_4 emitting) and methanotrophic (CH_4 consuming) communities, they may act as net CH_4 sources or sinks under certain conditions (Carmichael et al., 2024; Martinez et al., 2022). In the limited studies available on this topic, the balance between methanogenesis and methanotrophy in snags appears to be strongly influenced by moisture availability and oxygen levels (Terazawa et al., 2021). Thus, in drier, well-aerated upland conditions, methanotrophic activity may dominate, leading to CH_4 uptake; in contrast, in saturated lowlands or wetlands, anaerobic conditions support CH_4 production, leading to net emission.

Despite their clear contribution to GHG budgets of forests, differences in gas fluxes between living and dead tree stems remain poorly understood. CH_4 emissions are generally higher in living than dead stems, depending on stage of decay (Covey et al., 2016; Covey & Megonigal, 2019). CO_2 emissions from deadwood are typically higher than those from living stems, but smaller than soil emissions (Warner et al., 2017). Nonetheless, snags remain active sites of biogeochemical exchange of CO_2 and CH_4 due to their unique microbial composition. GHG fluxes may also co-vary in ways that reflect underlying environmental controls such as moisture and temperature. Thus, snags may represent a significant, yet often overlooked, component of GHG fluxes in forest ecosystems.

Here we describe CO_2 and CH_4 fluxes from repeated measurements on a series of snags along an upland-to-wetland gradient in a northern temperate conifer forest. Our objectives were to (1) identify the important drivers of CO_2 and CH_4 fluxes from snags, (2) illustrate how these fluxes respond to key environmental variables, and (3) determine if fluxes co-vary along an upland-to-wetland gradient. In doing so, we shed light on the importance of snags in ecosystem carbon dynamics, their dependence on environmental conditions, and their significance in GHG fluxes.

2 Methods

2.1 Site Description

This study was conducted at Howland Research Forest of central Maine, USA (45.2041°N 68.7402°W, elevation 60 m above sea level), located in the transition zone between deciduous and boreal forests in northeastern North America. The climate is damp and cool, with average annual temperatures of 5.9 ± 0.8°C and mean precipitation of 112 ± 21 cm/year that is evenly distributed throughout the year (Daly et al., 2008). Mean daily temperature ranged from -1.2 to 26.6 °C with an average of 15.2 °C from May to November, 2024, when this study took place. During this same period, daily precipitation ranged from 0 to 41.3 mm with a mean of 2.5 mm. Peak temperature occurred on August 2nd and peak precipitation occurred on August 9th.

The mature, multi-aged forest is composed of approximately 90% conifers, primarily red spruce (*Picea rubens*), which accounts for 51% of the site's basal area. The forest has not been actively managed since a partial harvest in the 1920s and now displays late-successional features, including large, old trees (over 200 years), a variety of tree diameters, and diverse stages of coarse woody debris decomposition (Fien et al., 2019). Soils in the area developed from coarse-loamy granitic

Deleted: In this technical note,

Deleted: clarify

basal till and vary in drainage from well-drained to poorly drained across short distances along upland-to-wetland transitions (Fernandez et al., 1993). Average soil organic layer depth at the six snags was 8 cm (Table A1). Snags account for roughly 35% (440 ± 20 g C m^{-2}) of deadwood

110   biomass and 3% of total aboveground biomass at this site (Hollinger et al., 2021).
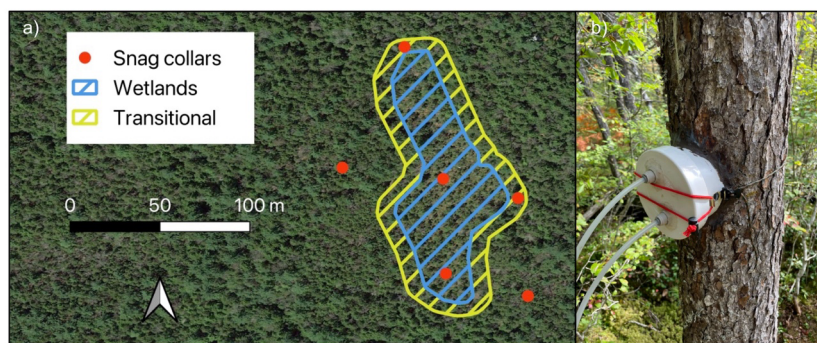
Figure 1: (a) Sampling collar locations for gas flux measurements throughout the designated wetlands, transitional areas, and uplands. (b) Chamber design with inlet and outlet tubes for connecting to a gas analyzer.

115

2.2 Data Collection

We randomly selected six standing dead red spruce stems for gas flux sampling (Hettwer et al., 2025a). The snags were within decay classes two and three, based on the five-class system of Sollins (1982), where one is recently dead wood and five is heavily decomposed. Snags spanned

120   an upland-to-wetland drainage gradient, where two were in uplands, two in transitional drainage, and two in an wetlands (Fig. 1). Drainage classes (wetland, transitional, upland) were assigned based on soil moisture data obtained from 100 randomly placed soil moisture sensors, as well as a National Wetlands Inventory wetland delineation. All analyses were conducted across continuous predictor variables (e.g., soil moisture, temperature); drainage classes were used solely to guide

125   snag selection and were not used as grouping factors in the data analyses.

To measure CO_2 and CH_4 flux from snag surfaces, we affixed custom-fitted PVC collars to snags with pure silicone at 50 cm stem height (Hettwer et al., 2025b). All collars were checked for leaks before each measurement by exhaling around the collar, with additional silicone applied as necessary. CO_2 and CH_4 concentrations were measured by sealing each collar with a custom PVC chamber lid, connected via 3 meters of 6.4 mm (¼-inch) Bev-A-Line tubing to a LI-7810 analyzer (LI-COR Biosciences, Lincoln, NE, USA). Ambient air was flushed through the system until gas concentrations stabilized, after which manual fluxes were recorded at a frequency of 1 Hz for six-minute intervals (Hutchinson et al., 2000) per observation and processed as described below. Fluxes were also periodically measured from a set of decay class two (N=6) and decay class four (N=6) *P. rubens* logs, decay class four *P. rubens* stumps (N=6), and soils according to the same protocol and at the same site.

While obtaining flux measurements from each snag, instantaneous air temperature was measured with radiation shielding (Precision Lollipop Digital Thermometer, Traceable), while soil moisture (%) and soil temperature were recorded at three locations around the snag at a depth of 15 cm (True TDR-315N Soil Moisture Sensor, Acclima). While we did not directly measure snag moisture, previous work has shown that snag volumetric water content closely tracks that of surface soil (Green et al., 2022). This makes soil moisture, a more widely available and routinely measured environmental variable, a reasonable proxy for snag moisture in our study. Flux and environmental data were collected every two weeks from May through November 2024, resulting in a total of 76 measurements. Hemispherical photographs were taken at three points around each snag (two meters from stem, at bearings 0, 120 and 240°) and processed using Gap Light Analyzer software (Frazer et al., 1999) to yield canopy openness values. Relative humidity was measured using a platinum resistance thermometer (EE181-L, Campbell Scientific) from an on-site flux

tower, with data scanned every minute and averaged over 30-minute intervals. For each flux measurement, the closest corresponding humidity measurement in time was selected.

2.3 Data Processing

Fluxes for CO_2 (μmol m^{-2} s^{-1}) and CH_4 (nmol m^{-2} s^{-1}) were calculated from the gas analyzer output using the ideal gas law (Equation 1), where $PV = nRT$ (P = barometric pressure, atm, V = chamber volume, L (liters), R (gas constant) = 0.08206 L·atm/mol·K, T = temperature, °C).

$$Flux = \left(\frac{dC}{dt}\right)\left(\frac{V}{A}\right)\frac{P}{(R*(T+273.15))}$$ (1)

The rate of change in gas concentration over time (dC/dt) was calculated from 90 to 345 seconds for each sampling event, using gas concentration versus time data obtained from the gas analyzer. This timeframe was chosen to reduce the influence of chamber sealing artifacts and initial concentration surges commonly seen in wetland trees (Yong et al., 2024). Barometric pressure (P) was paired with the nearest 30-minute measurement recorded by an on-site pressure sensor. Chamber volumes (V) were determined in the lab for each chamber size by sealing the tree-facing side with a contour-fitting cover, filling the chamber with quinoa seeds, and measuring the displaced volume. Surface areas (A) of tree stems within the chambers were also calculated for each template size. Air temperature (°C) at the time of sampling was converted to Kelvin (K) before calculating fluxes. The minimum detectable flux was estimated for each measurement following methods from Christiansen et al. (2015) and Nickerson (2016) with all measured fluxes falling within detectable limits. Data processing was performed in R (version 4.5.0) (R Core Team, 2024) using RStudio (Posit Team, 2024).

2.4 Data Analysis

To investigate the environmental drivers of CO_2 and CH_4 fluxes from snags, we conducted a series of statistical and predictive modeling approaches. Random forest analysis, using the *Boruta* package in R (Kursa and Rudnicki, 2010), allowed us to identify the most influential environmental predictors associated with each gas flux. These potential predictors included air temperature, soil temperature, volumetric soil moisture, relative humidity, organic soil pH, diameter at breast height, and canopy openness. We then used symbolic regression in Python (PySR) to determine mathematical models that best describe the relationships between top environmental predictors and gas fluxes (separate models for CO_2 and CH_4). This algorithm generated interpretable nonlinear models by automatically developing numerous candidate models and ranking them based on AICc scores (Cranmer, 2023).

To evaluate the strength of nonlinear interaction effects between predictor variables, we computed the second-order mixed partial derivatives ($\partial^2 y / \partial x_1 \partial x_2$) of the fitted nonlinear response surfaces. Doing so allowed us to assess how the effect of one predictor (e.g., soil moisture) on the response (e.g., CO_2 or CH_4 flux) changed depending on the level of another predictor (e.g., soil or air temperature). By calculating these interaction terms across a grid of observed data ranges, we identified regions where interactions were strongest, which may indicate synergistic or antagonistic environmental effects on gas fluxes. Given the response curve, we determined the optimal soil moisture (x_1) for maximizing CO_2 flux (y) by setting the derivative of $\ln(y)$ with respect to x_1 to 0 (Equation 2).

$$\frac{d}{dx_1}\ln(y) = ab - 2a\frac{x_1}{x_2} = 0 \ \rightarrow \ x_1 = \frac{bx_2}{2} \tag{2}$$

To determine if the relationship between CO_2 and CH_4 fluxes varied across the soil moisture gradient, we fit linear models with CH_4 flux as a response to the interaction between soil moisture

and CO_2 flux. For CO_2 and CH_4 fluxes in this two-gas model, we used our top-performing nonlinear models and held temperature constant at low (25th percentile) and high (75th percentile)

200 values. We then used a multivariate analysis of variance (MANOVA) to test whether soil moisture jointly influenced CO_2 and CH_4 fluxes, treating both gases as simultaneous response variables, at low and high temperatures. Lastly, we used Pearson tests on raw data to determine the correlation between CO_2 and CH_4 fluxes.

205 **3 Results**

Sampling period snag CO_2 fluxes ranged from 0.20 to 9.75 µmol m^{-2} s^{-1} (mean ± std. dev. = 2.26 ± 2.34) and CH_4 fluxes ranged from -0.21 to 2.46 nmol m^{-2} s^{-1} (0.25 ± 0.44). CO_2 emissions were highest from late-June to late-July and CH_4 emissions were highest from mid-July to mid-August
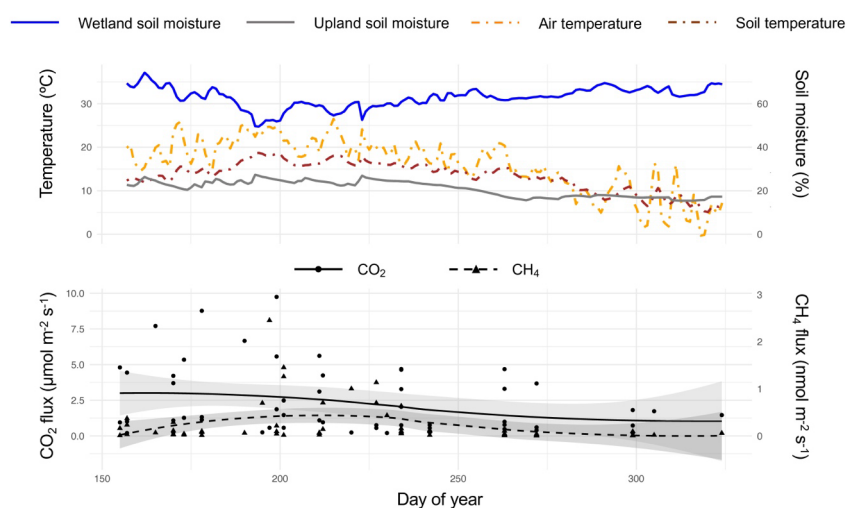
Figure 2: Top pane shows environmental conditions (temperature and soil moisture)
210 **throughout the sampling period, obtained from on-site eddy-covariance tower. Bottom pane shows observed CO_2 (primary y-axis) and CH_4 (secondary y-axis) fluxes vs. day of year. The shaded regions around each spline represent the 95% confidence interval, calculated using standard errors from the smoothing model.**

(Fig. 2). Minor CH_4 uptake was observed only three times out of 72 measurements throughout the sampling period, all of which occurred on upland snags. Mean CO_2 and CH_4 fluxes approached zero between October (day of year 275) and November. In comparing fluxes from various substrates at Howland Research Forest, upland snags emerged as the largest emitters of CO_2 (Table 1). Wetland snags were the second-largest emitter of CH_4 behind wetland soils.

Table 1: Summary of CO_2 and CH_4 fluxes from snags, logs, stumps, soils, and living tree stems during the 2024 growing season at Howland Research Forest in central Maine. Data for living tree stem (*Picea rubens)* fluxes is from Hettwer et. al, 2025a.

Substrate	CO_2 flux (μmol m^{-2} s^{-1}) (mean ± std. dev.)	CH_4 flux (nmol m^{-2} s^{-1}) (mean ± std. dev.)
Upland snags	2.53 ± 2.15	0.030 ± 0.020
Wetland snags	0.69 ± 0.47	0.47 ± 0.55
Decay class 2 logs	1.27 ± 1.13	0.016 ± 0.014
Decay class 4 logs	1.41 ± 1.13	-0.046 ± 0.10
Decay class 4 stumps	0.91 ± 0.88	-0.0031 ± 0.055
Upland soils	1.58 ± 0.83	-0.47 ± 0.47
Wetland soils	2.14 ± 1.91	289 ± 137
Upland living tree stems	0.41 ± 0.27	0.0090 ± 0.0063
Wetland living tree stems	0.68 ± 0.67	0.041 ± 0.083

Based on random forest analysis, soil moisture, air temperature, and canopy openness were deemed important for CO_2 flux, and soil moisture, soil temperature, and canopy openness for CH_4 flux. Canopy openness was strongly correlated with soil moisture (r = 0.74) and was therefore omitted from subsequent analyses. Relative humidity and stem diameter were classified as unimportant and were also omitted. Results from our nonlinear model fitting suggested that CO_2 flux followed an exponential increase or decrease depending on the relative values of soil moisture and air temperature (Table 2, Fig. 3a). Importantly, this model has the potential for negative, or antagonistic, interaction between predictors. CH_4 flux responded to soil moisture and soil

temperature as a rational function where flux changed slowly until soil moisture approached a critical value, above which it increased dramatically, although modulated by soil temperature (Table 2, Fig. 3b).

Deleted: ¶

Table 2: Top-performing nonlinear models for CO_2 flux (μmol m^{-2} s^{-1}) and CH_4 flux (nmol m^{-2} s^{-1}) from snags with the functional forms of each model, the estimated parameters, and associated coefficients of determination (R^2).

Deleted: 1

Response (y)	Predictors (x_1, x_2)	Model form	a	b	R^2
CO_2 flux	Soil moisture, Air temperature	$y = e^{a \cdot x_1 \cdot (b - \frac{x_1}{x_2})}$	0.0657	2.119	0.62
CH_4 flux	Soil moisture, Soil temperature	$y = \frac{x_2 + a}{b - x_1}$	-7.0015	89.999	0.90

Modeling based on partial derivatives highlighted distinct response surfaces for the two gases while revealing interactive effects between the predictors for each (Fig. 3). The highest CO_2 fluxes occurred at intermediate soil moisture levels (25 – 35% volumetric soil moisture) and elevated temperatures (> 20 °C). The strongest positive interaction for predicting CO_2 flux ($\partial^2 y / \partial x_1 \partial x_2 = 0.05 \frac{\mu\text{mol m}^{-2}\text{ s}^{-1}}{\%VWC \cdot °C}$) occurred at 27% soil moisture and 28 °C air temperature (maximum observed value). The strongest negative interaction occurred at 53% soil moisture and 28 °C air temperature. Assuming maximum observed air temperature, CO_2 flux reached its maximum at 30% volumetric soil moisture. The nonlinear models also highlight the relationship between CO_2 and CH_4 fluxes along the upland-to-wetland moisture gradient (Fig. 4). CO_2 flux peaked at approximately 30% soil moisture, then declined exponentially until becoming negligible at approximately 60% soil moisture, where CH_4 fluxes exhibited a sharp increase.

Formatted: Line spacing: Double
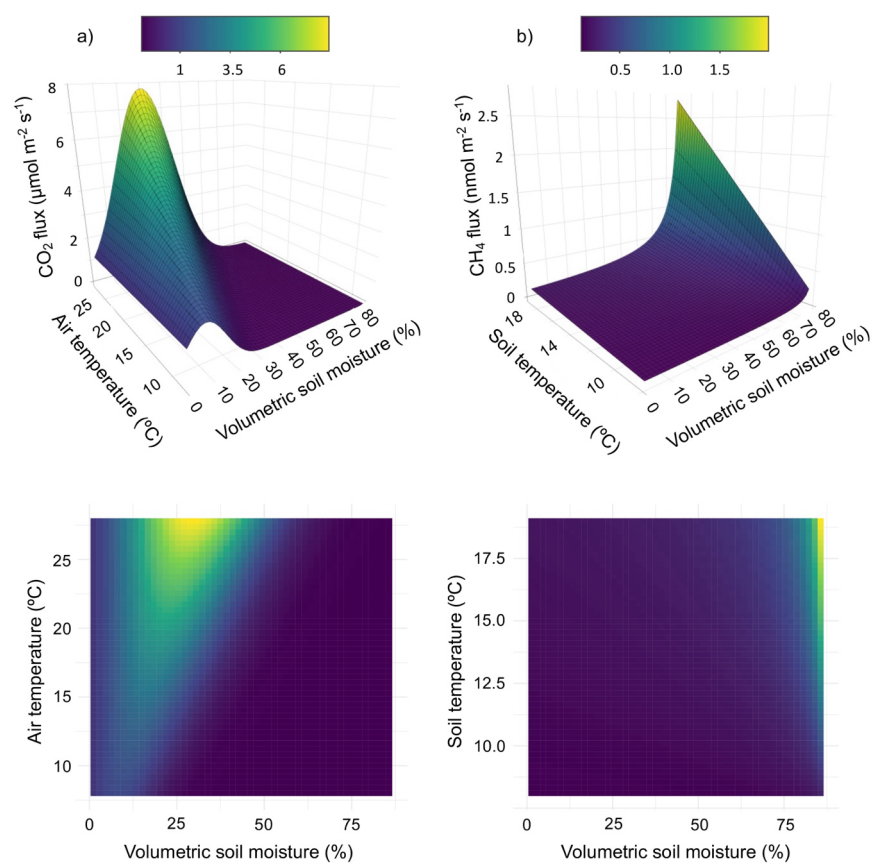
655 **Figure 3: Modeled relationships between (a) CO$_2$ and (b) CH$_4$ snag fluxes and top environmental variables, highlighting the important interactions between predictors for each gas. Color scales correspond to CO$_2$ (μmol m^{-2} s^{-1}) and CH$_4$ (nmol m^{-2} s^{-1}) units. Top pane shows 3D surface plots and bottom pane shows 2D heatmaps.**
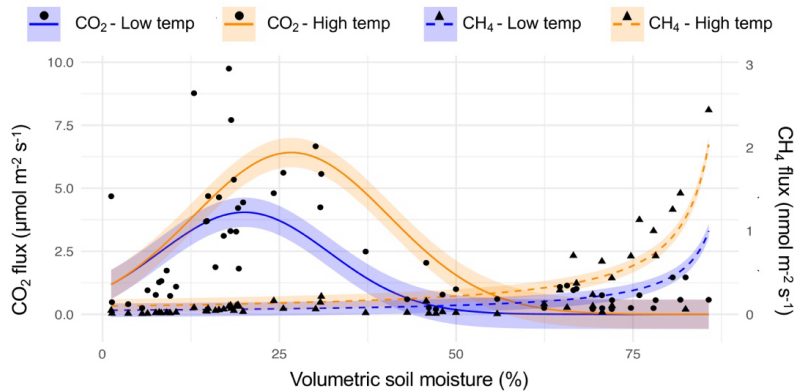
660 **Figure 4: Observed snag CO_2 and CH_4 fluxes along a soil-moisture gradient, with curve fits corresponding to top-performing nonlinear models. Temperature (air temperature for CO_2, soil temperature for CH_4) was held constant at low (25th percentile) and high (75th percentile) values for predicting curves. Shaded regions around each curve represent the 95% confidence intervals.**

665 CH_4 fluxes increased sharply with higher soil moisture levels (~ 60%) and exhibited negligible

response to increases in soil temperature, except when soil moisture was high. The strongest

interaction effect between predictors was observed at 86% soil moisture (maximum observed

value) and 17 °C soil temperature, while the weakest interaction occurred at 1% soil moisture

(minimum observed value) and 14 °C soil temperature.

670 The two-gas model revealed a significant negative interaction between CO_2 flux and soil moisture

in predicting CH_4 flux (p < 0.001), indicating that the positive effect of soil moisture on CH_4 flux

weakened as CO_2 flux increased. Regardless of temperature percentile, the relationship between

the two gases varied along the soil moisture gradient. Specifically, CH_4 flux increased when CO_2

flux decreased under increasing moisture conditions. Furthermore, the MANOVA results show that

675 CO_2 and CH_4 fluxes were jointly influenced by soil moisture (p < 0.001). CH_4 and CO_2 fluxes were

negatively correlated (r = -0.53), suggesting they respond differently along the soil moisture gradient.

705

4 Discussion

Our results highlight the strong influence that soil moisture and temperature exert on gas fluxes from snags, demonstrating these responses along an upland-to-wetland moisture gradient. CO_2 fluxes peaked at intermediate soil moisture ($\sim$ 30%) and high temperatures, showing a significant

710 interaction between soil moisture and air temperature. CH_4 fluxes rose sharply at high soil moisture ($\sim$ 60%) and were primarily driven by soil moisture, with a strong interaction between soil moisture and soil temperature. These drivers, identified by random forest, make sense based on the differing origins of the emissions. CO_2 emissions are primarily a product of aerobic microbial respiration within the deadwood itself, and are therefore more influenced by air temperature. In contrast, CH_4

715 flux results from anaerobic methanogenesis in the saturated soils at the snag base, with the gas then transported up through the snag stem (Covey et al., 2016).

Formatted: Font: Times New Roman, Font color: Auto, Pattern: Clear

CO_2 flux increased as air temperature increased, in agreement with previous studies (Boddy, 1983; Noh et al., 2019), but it also depended on soil moisture. As soil moisture deviated in either direction from that of maximum CO_2 flux ($\sim$ 30%), flux decreased towards zero. Therefore, our results

720 suggest that fungal activity in snags, and in turn CO_2 emissions, may be inhibited at both low and high moisture conditions. The finding of reduced deadwood CO_2 flux under low moisture conditions has been reported in previous studies (Boddy, 1983; Hicks et al., 2003). The finding of reduced CO_2 flux at high moisture conditions corroborates several deadwood studies (Meyer and Brischke, 2015; Progar et al., 2000) but contrasts with others (Forrester et al., 2012; Gough et al.,

725 2007).

CH$_4$ flux increased sharply with rising soil moisture when soil temperature was high, indicating a synergistic effect between the two variables. Similarly, CH$_4$ flux became more responsive to increases in soil temperature when soil moisture was high, suggesting that optimal conditions for CH$_4$ emission occurred when both predictors were elevated. CH$_4$ flux rates, as well as interaction effects of predictor variables, were negligible in drier, cooler conditions. The insensitivity of CH$_4$ flux to increasing soil moisture, even at high temperatures, aligns with findings of a volumetric soil moisture threshold of $\sim 60\%$ beyond which CH$_4$ flux rates from soils increase dramatically (von Fischer and Hedin, 2007). While a positive relationship between CH$_4$ flux and moisture has been observed from soils and other deadwood forms (Covey & Megonigal, 2019; Kipping et al., 2022), the dynamics of snag CH$_4$ flux and its dependence on moisture remain poorly understood, perhaps due to the challenge of directly measuring internal snag moisture (Green et al., 2022).

Our results point to a complex, moisture-sensitive relationship between CO$_2$ and CH$_4$ fluxes in the studied ecosystem. The significant interaction between CO$_2$ flux and soil moisture in predicting CH$_4$ flux suggests that the behavior of one gas flux may be linked to the other, especially under varying moisture conditions. As soil moisture increased, CO$_2$ flux declined while CH$_4$ flux rose, indicating a possible transition from aerobic to anaerobic microbial processes. The negative correlation between CO$_2$ and CH$_4$ fluxes, combined with MANOVA results showing soil moisture as a joint flux driver, reinforces the assumption that the coupling of these gas fluxes is moisture dependent. Furthermore, the shift in positive CO$_2$ to CH$_4$ fluxes between $60 - 70\%$ moisture aligns with reported values for volumetric water content at which conditions shift from aerobic to anaerobic (Długosz et al., 2024; Fairbairn et al., 2023; Schlüter et al., 2025). Overall, these findings underscore the importance of soil moisture in regulating greenhouse gas dynamics in forested

systems and the value of using a two-gas framework to understand GHG fluxes as they pertain to radiative forcing and climate change.

In addition to exhibiting uniquely complex relationships between gas fluxes and environmental drivers, snags may also emit higher rates of CO_2 and CH_4 than other forest surfaces. Several studies report that snags can emit CO_2 and CH_4 at rates comparable to or greater than those from downed wood and live trees. Martinez et al. (2022) measured average wetland snag flux rates of 0.73 μmol CO_2 m^{-2} s^{-1} and 5.21 nmol CH_4 m^{-2} s^{-1}, and Carmichael et al. (2018) measured 0.72 μmol CO_2 m^{-2} s^{-1} and 6.94 nmol CH_4 m^{-2} s^{-1}. While snag CH_4 emissions were not this large at our site, they still exceeded those from living trees, revealing a pattern not previously documented. Emphasized by their magnitude of CO_2 and CH_4 fluxes and relationships with environmental predictors, snags represent an important and understudied component of forest biogeochemical exchange, particularly across drainage gradients where CO_2 and CH_4 emissions will vary independently.

In summary, we found that moisture and temperature interact in complex ways to govern both CO_2 and CH_4 fluxes from snags. Both gas fluxes increased with increasing temperature, yet CO_2 flux peaked at moderate moisture levels, while CH_4 peaked at the highest moisture recorded. CH_4 fluxes were overwhelmingly net positive (i.e., sources to the atmosphere), suggesting that snags represent an important pathway for wetland gas production; however, they may serve as CH_4 sinks under certain conditions. Our results derive from a small number of snags, yet they provide compelling evidence for the importance of snag fluxes in the forest carbon cycle, particularly considering projected increases in regional temperature and precipitation (Fernandez et al., 2020). Our results identify further knowledge gaps regarding the influence of snag wood traits, stem height, stages of snag decay, and fungal community composition.

Conclusions

These results demonstrate that standing dead trees (snags) in northern conifer forests emit both CO_2 and CH_4, with flux dynamics strongly regulated by environmental gradients, particularly soil moisture. CO_2 flux peaked at intermediate soil moisture ($\sim 30\%$) and warm air temperatures, following a rational response shaped by interactive effects between soil moisture and air temperature. In contrast, CH_4 flux remained low until soil moisture exceeded a threshold ($\sim 60\%$), after which emissions increased sharply, modulated by soil temperature. The observed negative correlation between CO_2 and CH_4 fluxes, along with evidence of an interaction between CO_2 flux and soil moisture in predicting CH_4 flux, suggests that the two gases respond divergently along the upland-to-wetland gradient. Overall, these findings highlight the complexity of greenhouse gas emissions from snags and underscore the importance of considering interactive environmental drivers when modeling their contributions to forest carbon dynamics.

Appendix A

Table A1: Organic layer depth (mean of three points) for each snag and mean soil moisture and snag fluxes across the sampling period. Also reported are the standard deviations for soil moisture, CH_4 flux, and CO_2 flux.

Snag	Mean soil organic layer depth (cm)	Mean soil moisture (%)	Mean CH_4 flux (nmol $m^{-2} s^{-1}$)	Mean CO_2 flux (μmol $m^{-2} s^{-1}$)
1	7.62	67.9 ± 12.9	0.628 ± 0.708	0.536 ± 0.492
2	10.16	64.4 ± 12.9	0.493 ± 0.444	0.875 ± 0.395
3	8.23	19.2 ± 9.5	0.085 ± 0.028	5.070 ± 3.040
4	9.53	23.1 ± 5.7	0.133 ± 0.043	3.890 ± 1.220
5	5.56	7.46 ± 4.2	0.017 ± 0.011	0.933 ± 0.519
6	6.99	15.6 ± 6.9	0.045 ± 0.017	4.590 ± 1.580

Data availability

815 The datasets generated and analyzed during the current study have been made available in the Environmental Data Initiative (EDI) repository. Refer to the citation for Hettwer et al., 2025b in the references.

Competing interests

820 The authors declare that they have no conflicts of interest.

Acknowledgements

We would like to thank Ivan Fernandez, Jonathan Gewirtzman, and Rachel Poppe for their help with this manuscript. This research was supported in part by the U.S. National Science Foundation

825 (DEB Award #2208658, 2208655), the U.S. Department of Energy's Office of Science (AmeriFlux core site), the U.S. Forest Service, Northern Research Station (JVA #25-JV-11242306-009), and the Maine Agricultural and Forest Experiment Station (ME042612, ME042121).

830 **Author contributions**

All authors contributed to the study conception and design. Material preparation, data collection and analysis were performed by Christian Hettwer. The first draft of the manuscript was written by Christian Hettwer and all authors commented on previous versions of the manuscript. All authors read and approved the final manuscript.

835 **References**

Barba, J., Bradford, M. A., Brewer, P. E., Bruhn, D., Covey, K., van Haren, J., Megonigal, J. P., Mikkelsen, T. N., Pangala, S. R., Pihlatie, M., Poulter, B., Rivas-Ubach, A., Schadt, C. W., Terazawa, K., Warner, D. L., Zhang, Z., and Vargas, R.: Methane emissions from tree
840   stems: a new frontier in the global carbon cycle, New Phytologist, 222, 18–28, https://doi.org/https://doi.org/10.1111/nph.15582, 2019.

Boddy, L.: Carbon dioxide release from decomposing wood: Effect of water content and temperature, Soil Biol Biochem, 15, 501–510, https://doi.org/https://doi.org/10.1016/0038-0717(83)90042-1, 1983.

845 Carmichael, M. J., Helton, A. M., White, J. C., and Smith, W. K.: Standing Dead Trees are a Conduit for the Atmospheric Flux of CH4 and CO2 from Wetlands, Wetlands, 38, 133–143, https://doi.org/10.1007/s13157-017-0963-8, 2018.

Carmichael, M. J., Martinez, M., Bräuer, S. L., and Ardón, M.: Microbial Communities in Standing Dead Trees in Ghost Forests are Largely Aerobic, Saprophytic, and
850   Methanotrophic, Curr Microbiol, 81, 229, https://doi.org/10.1007/s00284-024-03767-w, 2024.

Christiansen, J., Outhwaite, J., and Smukler, S.: Comparison of CO2, CH4 and N2O soil-atmosphere exchange measured in static chambers with cavity ring-down spectroscopy and gas chromatography, Agric For Meteorol, 211,
855   https://doi.org/10.1016/j.agrformet.2015.06.004, 2015.

Conrad, R.: Methane Production in Soil Environments—Anaerobic Biogeochemistry and Microbial Life between Flooding and Desiccation, Microorganisms, 8, 881, https://doi.org/10.3390/microorganisms8060881, 2020.

Covey, K. R. and Megonigal, J. P.: Methane production and emissions in trees and forests, New
860   Phytologist, 222, 35–51, https://doi.org/10.1111/nph.15624, 2019.

Covey, K. R., de Mesquita, C. P. B., Oberle, B., Maynard, D. S., Bettigole, C., Crowther, T. W., Duguid, M. C., Steven, B., Zanne, A. E., Lapin, M., Ashton, M. S., Oliver, C. D., Lee, X., and Bradford, M. A.: Greenhouse trace gases in deadwood, Biogeochemistry, 130, 215–226, https://doi.org/10.1007/s10533-016-0253-1, 2016.

865 Cranmer, M.: Interpretable Machine Learning for Science with PySR and SymbolicRegression.jl, https://arxiv.org/abs/2305.01582, 2023.

Daly, C., Halbleib, M. D., Smith, J. I., Gibson, W., Doggett, M. K., Taylor, G. H., Curtis, J. M., and Pasteris, P. P.: Physiographically sensitive mapping of climatological temperature and precipitation across the conterminous United States, International Journal of Climatology,
870   28, 2031–2064, https://doi.org/10.1002/joc.1688, 2008.

Długosz, J., Piotrowska-Długosz, A., and Breza-Boruta, B.: The effect of differences in soil water content on microbial and enzymatic properties across the soil profiles, Ecohydrology & Hydrobiology, 24, 547–556, https://doi.org/https://doi.org/10.1016/j.ecohyd.2023.06.010, 2024.

875 Fairbairn, L., Rezanezhad, F., Gharasoo, M., Parsons, C. T., Macrae, M. L., Slowinski, S., and Van Cappellen, P.: Relationship between soil CO2 fluxes and soil moisture: Anaerobic sources explain fluxes at high water content, Geoderma, 434, 116493, https://doi.org/https://doi.org/10.1016/j.geoderma.2023.116493, 2023.

Fernandez, I. J., Son, Y., Kraske, C. R., Rustad, L. E., and David, M. B.: Soil Carbon Dioxide
880   Characteristics under Different Forest Types and after Harvest, Soil Science Society of

America Journal, 57, 1115–1121,
https://doi.org/https://doi.org/10.2136/sssaj1993.03615995005700040039x, 1993.

Fernandez, I. J., Birkel, S., Schmitt, C. V, Simonson, J., Lyon, B., Pershing, A., Stancioff, E., and
Jacobson, G. L.: Maine's climate future: 2020 update,
https://doi.org/10.13140/RG.2.2.24401.07521, 2020.

Fien, E. K. P., Fraver, S., Teets, A., Weiskittel, A. R., and Hollinger, D. Y.: Drivers of individual
tree growth and mortality in an uneven-aged, mixed-species conifer forest, For Ecol
Manage, 449, 117446, https://doi.org/10.1016/j.foreco.2019.06.043, 2019.

von Fischer, J. C. and Hedin, L. O.: Controls on soil methane fluxes: Tests of biophysical
mechanisms using stable isotope tracers, Global Biogeochem Cycles, 21, GB2007,
https://doi.org/https://doi.org/10.1029/2006GB002687, 2007.

Forrester, J., Mladenoff, D., Gower, S., and Stoffel, J.: Interactions of temperature and moisture
with respiration from coarse woody debris in experimental forest canopy gaps, For Ecol
Manage, 265, 124–132, https://doi.org/10.1016/j.foreco.2011.10.038, 2012.

Frazer, G. W., Canham, C. D., and Lertzman, K. P.: Gap Light Analyzer (GLA), Version 2.0:
Imaging software to extract canopy structure and gap light transmission indices from true-
colour fisheye photographs, users manual and program documentation, 1999.

Gough, C., Vogel, C., Kazanski, C., Nagel, L., Flower, C., and Curtis, P.: Coarse woody debris
and the carbon balance of a north temperate forest, For Ecol Manage, 244, 60–67,
https://doi.org/10.1016/j.foreco.2007.03.039, 2007.

Green, M. B., Fraver, S., Lutz, D. A., Woodall, C. W., D'Amato, A. W., and Evans, D. M.: Does
deadwood moisture vary jointly with surface soil water content?, Soil Science Society of
America Journal, 86, 1113–1121, https://doi.org/https://doi.org/10.1002/saj2.20413, 2022.

Hararuk, O., Kurz, W. A., and Didion, M.: Dynamics of dead wood decay in Swiss forests, For
Ecosyst, 7, 36, https://doi.org/10.1186/s40663-020-00248-x, 2020.

Hettwer, C., Savage, K., Gewirtzman, J., Ruzol, R., Wason, J., Cadillo-Quiroz, H., and Fraver,
S.: Methane flux from living tree stems in a northern conifer forest, Biogeochemistry, 168,
66, https://doi.org/10.1007/s10533-025-01257-0, 2025a.

Hettwer, C., Fraver, S., and Savage, K.: CO2 and CH4 fluxes from living and standing dead trees
in Howland Research Forest, Maine USA, 2024, Environmental Data Initiative,
https://doi.org/https://doi.org/10.6073/pasta/03586624214245c96a0399509ab4e3cb, 2025b.

Hicks, W., Harmon, M., and Griffiths, R.: Abiotic controls on nitrogen fixation and respiration in
selected woody debris from the Pacific Northwest, U.S.A, Ecoscience, 10, 66–73,
https://doi.org/10.1080/11956860.2003.11682752, 2003.

Hollinger, D. Y., Davidson, E. A., Fraver, S., Hughes, H., Lee, J. T., Richardson, A. D., Savage,
K., Sihi, D., and Teets, A.: Multi-Decadal Carbon Cycle Measurements Indicate Resistance
to External Drivers of Change at the Howland Forest AmeriFlux Site, J Geophys Res
Biogeosci, 126, e2021JG006276, https://doi.org/10.1029/2021JG006276, 2021.

Hutchinson, G. L., Livingston, G. P., Healy, R. W., and Striegl, R. G.: Chamber measurement of
surface-atmosphere trace gas exchange: Numerical evaluation of dependence on soil,
interfacial layer, and source/sink properties, Journal of Geophysical Research:
Atmospheres, 105, 8865–8875, https://doi.org/https://doi.org/10.1029/1999JD901204,
2000.

Keppler, F., Hamilton, J. T. G., Braß, M., and Röckmann, T.: Methane emissions from terrestrial
plants under aerobic conditions, Nature, 439, 187–191,
https://doi.org/10.1038/nature04420, 2006.

Kipping, L., Gossner, M. M., Koschorreck, M., Muszynski, S., Maurer, F., Weisser, W. W., Jehmlich, N., and Noll, M.: Emission of CO2 and CH4 From 13 Deadwood Tree Species Is Linked to Tree Species Identity and Management Intensity in Forest and Grassland
930   Habitats, Global Biogeochem Cycles, 36, e2021GB007143, https://doi.org/10.1029/2021GB007143, 2022.

Komposch, A., Ensslin, A., Fischer, M., and Hemp, A.: Aboveground Deadwood Biomass and Composition Along Elevation and Land-Use Gradients at Mount Kilimanjaro, Front Ecol Evol, 9, https://doi.org/10.3389/fevo.2021.732092, 2022.

935   Kursa, M. B. and Rudnicki, W. R.: Feature Selection with the Boruta Package, J Stat Softw, 36, 1–13, https://doi.org/10.18637/jss.v036.i11, 2010.

Martinez, M., Ardón, M., and Carmichael, M. J.: Identifying Sources and Oxidation of Methane in Standing Dead Trees in Freshwater Forested Wetlands, Front Environ Sci, 9, https://doi.org/10.3389/fenvs.2021.737379, 2022.

940   Meyer, L. and Brischke, C.: Fungal decay at different moisture levels of selected European-grown wood species, Int Biodeterior Biodegradation, 103, 23–29, https://doi.org/https://doi.org/10.1016/j.ibiod.2015.04.009, 2015.

Mukhortova, L., Pashenova, N., Meteleva, M., Krivobokov, L., and Guggenberger, G.: Temperature sensitivity of CO2 and CH4 fluxes from coarse woody debris in northern
945   boreal forests, Forests, 12, 624, https://doi.org/10.3390/f12050624, 2021.

Nickerson, N.: Evaluating gas emission measurements using Minimum Detectable Flux (MDF), https://doi.org/10.13140/RG.2.1.4149.2089, 2016.

Noh, N. J., Shannon, J. P., Bolton, N. W., Davis, J. C., Van Grinsven, M. J., Pypker, T. G., Kolka, R. K., and Wagenbrenner, J. W.: Temperature responses of carbon dioxide fluxes from
950   coarse dead wood in a black ash wetland, Wetl Ecol Manag, 27, 157–170, https://doi.org/10.1007/s11273-018-9649-0, 2019.

Oberle, B., Ogle, K., Zanne, A., and Woodall, C.: When a tree falls: Controls on wood decay predict standing dead tree fall and new risks in changing forests, PLoS One, 13, e0196712, https://doi.org/10.1371/journal.pone.0196712, 2018.

955   Olajuyigbe, S., Tobin, B., and Nieuwenhuis, M.: Temperature and moisture effects on respiration rate of decomposing logs in a Sitka spruce plantation in Ireland, Forestry: An International Journal of Forest Research, 85, 485–496, https://doi.org/10.1093/forestry/CPS045, 2012.

Onega, T. L. and Eickmeier, W. G.: Woody Detritus Inputs and Decomposition Kinetics in a Southern Temperate Deciduous Forest, Bulletin of the Torrey Botanical Club, 118, 52–57,
960   https://doi.org/10.2307/2996975, 1991.

Pangala, S. R., Moore, S., Hornibrook, E. R. C., and Gauci, V.: Trees are major conduits for methane egress from tropical forested wetlands, New Phytologist, 197, 524–531, https://doi.org/10.1111/nph.12031, 2013.

Pangala, S. R., Hornibrook, E. R. C., Gowing, D. J., and Gauci, V.: The contribution of trees to
965   ecosystem methane emissions in a temperate forested wetland, Glob Chang Biol, 21, 2642–2654, https://doi.org/10.1111/gcb.12891, 2015.

Perreault, L., Forrester, J. A., Mladenoff, D. J., and Gower, S. T.: Linking deadwood and soil GHG fluxes in a second growth north temperate deciduous forest (Upper Midwest USA), Biogeochemistry, 156, 177–194, https://doi.org/10.1007/s10533-021-00839-y, 2021.

970   Posit Team: RStudio: Integrated Development Environment for R, https://posit.co/, 2024.

Progar, R. A., Schowalter, T. D., Freitag, C. M., and Morrell, J. J.: Respiration from coarse woody debris as affected by moisture and saprotroph functional diversity in Western Oregon, Oecologia, 124, 426–431, https://doi.org/10.1007/PL00008868, 2000.

R Core Team: R: A language and environment for statistical computing, https://www.R-project.org/, 2024.

Renninger, H. J., Carlo, N., Clark, K. L., and Schäfer, K. V. R.: Modeling respiration from snags and coarse woody debris before and after an invasive gypsy moth disturbance, J Geophys Res Biogeosci, 119, 630–644, https://doi.org/https://doi.org/10.1002/2013JG002542, 2014.

Russell, M. B., Fraver, S., Aakala, T., Gove, J. H., Woodall, C. W., D'Amato, A. W., and Ducey, M. J.: Quantifying carbon stores and decomposition in dead wood: A review, For Ecol Manage, 350, 107–128, https://doi.org/10.1016/j.foreco.2015.04.033, 2015.

Schlüter, S., Lucas, M., Grosz, B., Ippisch, O., Zawallich, J., He, H., Dechow, R., Kraus, D., Blagodatsky, S., Senbayram, M., Kravchenko, A., Vogel, H.-J., and Well, R.: The anaerobic soil volume as a controlling factor of denitrification: a review, Biol Fertil Soils, 61, 343–365, https://doi.org/10.1007/s00374-024-01819-8, 2025.

Sollins, P.: Input and decay of coarse woody debris in coniferous stands in western Oregon and Washington, Canadian Journal of Forest Research, 12, 18–28, https://doi.org/10.1139/x82-003, 1982.

Terazawa, K., Tokida, T., Sakata, T., Yamada, K., and Ishizuka, S.: Seasonal and weather-related controls on methane emissions from the stems of mature trees in a cool-temperate forested wetland, Biogeochemistry, 156, 1–20, https://doi.org/10.1007/s10533-021-00841-4, 2021.

Warner, D. L., Villarreal, S., McWilliams, K., Inamdar, S., and Vargas, R.: Carbon Dioxide and Methane Fluxes From Tree Stems, Coarse Woody Debris, and Soils in an Upland Temperate Forest, Ecosystems, 20, 1205–1216, https://doi.org/10.1007/s10021-016-0106-8, 2017.

Woodall, C. W., Russell, M. B., Walters, B. F., D'Amato, A. W., Fraver, S., and Domke, G. M.: Net carbon flux of dead wood in forests of the Eastern US, Oecologia, 177, 861–874, https://doi.org/10.1007/s00442-014-3171-8, 2015.

Yatskov, M. A., Harmon, M. E., Fasth, B., Sexton, J., Hoyman, T. L., and Dudoit, C. M.: Decomposition differences between snags and logs in forests of Kenai Peninsula, Alaska, Canadian Journal of Forest Research, 52, 727–742, https://doi.org/10.1139/cjfr-2021-0208, 2022.

Yong, Z.-J., Lin, W.-J., Lin, C.-W., and Lin, H.-J.: Tidal influence on carbon dioxide and methane fluxes from tree stems and soils in mangrove forests, Biogeosciences, 21, 5247–5260, https://doi.org/10.5194/bg-21-5247-2024, 2024.